AGU PUBLICATIONS

Geophysical Research Letters

RESEARCH LETTER
10.1002/2013GL058842

Key Points:
- South Pacific shows stronger coupling to tropics than North Pacific via the PMMs
- The hemispheric asymmetry of the PMMs is mainly due to asymmetric mean trades
- Modulation of the mean state asymmetry can impact tropical Pacific variability

Correspondence to:
H. Zhang,
hzhang@rsmas.miami.edu

Citation:
Zhang, H., C. Deser, A. Clement, and R. Tomas (2014), Equatorial signatures of the Pacific Meridional Modes: Dependence on mean climate state, *Geophys. Res. Lett.*, *41*, 568–574, doi:10.1002/2013GL058842.

Received 26 NOV 2013
Accepted 8 JAN 2014
Accepted article online 13 JAN 2014
Published online 27 JAN 2014

Equatorial signatures of the Pacific Meridional Modes: Dependence on mean climate state

Honghai Zhang[1], Clara Deser[2], Amy Clement[1], and Robert Tomas[2]

[1]Rosenstiel School of Marine and Atmospheric Science, University of Miami, Miami, Florida, USA, [2]Climate Analysis, Climate and Global Dynamics, National Center for Atmospheric Research, Boulder, Colorado, USA

Abstract Extratropical atmospheric variability can impact tropical climate in the Pacific sector via the Pacific Meridional Modes (PMMs). The South PMM (SPMM) has a larger equatorial signature than the North PMM (NPMM) for the same amount of extratropical variability. Here we explain this interhemispheric asymmetry using an atmospheric general circulation model coupled to a slab ocean model. By imposing an anomalous interhemispheric heating gradient, we strengthen the northeasterly trades and weaken the southeasterly trades, shifting the Intertropical Convergence Zone south of the equator. As a result, the SPMM no longer influences the equatorial region while the NPMM shows strengthened linkages to the central-western equatorial Pacific. By demonstrating that background winds determine the propagation of the wind-evaporation-sea surface temperature feedback fundamental for the PMMs, we conclude that the interhemispheric asymmetry between the PMMs is largely attributed to the asymmetric mean trades in the Pacific. The results have implications for both paleoclimate studies and model development.

1. Introduction

The "Meridional Mode" represents a set of physical processes through which extratropical atmospheric variability influences tropical climate variability [e.g., *Chiang and Vimont*, 2004; *Zhang et al*., 2014], including Atlantic hurricane activity [*Kossin and Vimont*, 2007] and El Niño–Southern Oscillation (ENSO) [*Chang et al*., 2007]. A comprehensive physical understanding of the Meridional Mode is thus of both scientific and practical importance. The Meridional Mode involves the following set of processes: A weakening of the subtropical trade winds in association with extratropical variability warms the local sea surface temperature (SST) by modifying the turbulent heat flux (note that a strengthening of the winds has the opposite effect). The anomalous SST signal then propagates along the direction of the climatological trade winds via the wind-evaporation-SST (WES) feedback mechanism [*Xie and Philander*, 1994], resulting in a corresponding warm tropical SST anomaly. Cloud radiative feedback may amplify the SST anomaly in the eastern basin but are not required for the existence of the Meridional Mode [*Zhang et al*., 2014].

The Meridional Mode was identified first in the Atlantic [*Nobre and Shukla*, 1996; *Chang et al*., 1997] and then in the North Pacific [*Chiang and Vimont*, 2004]. Operating on seasonal-to-decadal time scales, these Meridional Modes are driven by extratropical atmospheric internal variability known as the North Atlantic Oscillation [e.g., *Xie and Tanimoto*, 1998] and North Pacific Oscillation [*Chiang and Vimont*, 2004], respectively. With evidence from both observations and climate models of different complexity, *Zhang* et al. [2014, hereafter ZCD13] have recently showed that a similar Meridional Mode also exists in the South Pacific.

Despite the similarities between the North Pacific Meridional Mode (NPMM) and the South Pacific Meridional Mode (SPMM), ZCD13 highlighted a key difference, namely, the interhemispheric asymmetry in their spatial structure. The NPMM is largely confined to the Northern Hemisphere with some influence on the northwestern tropical Pacific, while the SPMM exhibits much larger impact on the eastern-to-central equatorial Pacific. As a result, the SPMM leads to thermodynamic ENSO-like variability [*Clement et al*., 2011] and may even trigger dynamical ENSO events [ZCD13]. This difference between the NPMM and the SPMM is consistent with the model-based findings of *Matei et al*. [2008] and *Okumura* [2013]. *Matei et al*. [2008] found that the subtropical South Pacific has a larger and faster impact on the tropical Pacific through the atmosphere-ocean mixed layer interaction (akin to the SPMM), while the impact from the subtropical North Pacific is weaker and slower and arises via the oceanic meridional overturning circulation. *Okumura* [2013] argued that tropical Pacific decadal variability originates primarily from the Pacific/South American pattern over the South Pacific,

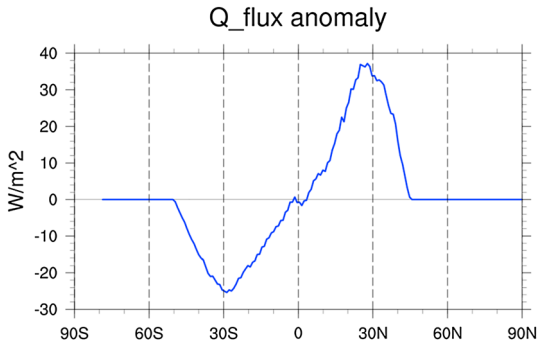

Figure 1. Q_{flux} anomaly (W/m^2) added to the SOM in the control run as a function of latitude. Positive values (heat divergence) denote cooling of the ocean ($dT/dt = Q_{net} - Q_{flux}$). See the text for its derivation.

with little contribution from the corresponding Pacific/North American pattern over the North Pacific. The physics underlying these decadal extratropical-to-tropical linkages are similar to the PMMs.

To explain the interhemispheric asymmetry between the two PMMs, ZCD13 hypothesized that it is due to the asymmetric mean surface winds in the tropical Pacific, whose distribution determines the spatial extent of the WES feedback [*Liu and Xie*, 1994]. The climatological southeast trade winds in the eastern Pacific cross the equator and converge with the northeast trade winds at the Intertropical Convergence Zone (ITCZ) around 7°N, favoring a stronger connection between the SPMM and the eastern equatorial Pacific while confining the NPMM to the north of the ITCZ. This hypothesis has theoretical support from two analytical studies, *Liu and Xie* [1994] and *Wang* [2010]. *Liu and Xie* [1994] explored the equatorward propagation of extratropical annual variability in a simplified Lindzen-Nigam atmospheric model coupled to an oceanic mixed layer model including partial ocean dynamics such as entrainment and advection. They demonstrated that the wave speed of the meridional propagation induced by the entrainment-evaporation process (similar to the WES feedback) is directly proportional to the mean meridional surface winds, which implies that the distribution of the mean meridional winds determines the spatial extent of the meridional propagation. *Wang* [2010] investigated thermodynamically coupled modes of variability in the tropics by analytically solving an idealized Gill-type model coupled to a slab ocean (no ocean dynamics). They found that cross-equatorial winds can introduce asymmetry to the analytical solutions that would otherwise be symmetric about the equator.

In this study, we will apply a state-of-the-art atmospheric general circulation model coupled to a slab ocean mixed layer model (AGCM-slab model) to test the hypothesis proposed by ZCD13. Compared to the idealized deterministic atmosphere models in *Liu and Xie* [1994] and *Wang* [2010], the AGCM includes much more sophisticated physics aimed for a more realistic climate simulation, and in particular, it allows stochastic forcing (e.g., intrinsic atmospheric variability independent of SST). The strategy is to modify the mean surface wind distribution in the tropical Pacific and examine the sensitivity of the equatorial impacts of the PMMs to the interhemispheric asymmetries in the background climate state. A simple conceptual model is also constructed to analytically support the conclusions drawn from the climate model experiments.

2. Experimental Design

We employ the standard slab ocean configuration of the Community Climate System Model version 4 (CCSM4) [*Gent et al.*, 2011], in which the active Community Atmosphere Model version 4 (CAM4), Community Land Model version 4 (CLM4), and the sea ice component version 4 (CICE4) are coupled to a slab ocean model (SOM) (labeled CAM4SOM) [*Bitz et al.*, 2012]. This AGCM-slab ocean configuration has proven capable of simulating the SPMM and NPMM in ZCD13. In CAM4SOM, both the prescribed ocean heat transport convergence (termed Q_{flux}) that compensates for the missing ocean dynamics and the depth of the slab ocean are derived from a 20 year preindustrial control run of the fully coupled CCSM4. The Q_{flux} field has a repeating seasonal cycle and is used to force the SST climatology toward that of the CCSM4. The depth of the slab ocean varies in space but is constant in time. In CAM4, all external forcings such as greenhouse gas concentrations and solar insolation are set to their preindustrial values. A detailed description of this CAM4SOM configuration can be found in *Bitz et al.* [2012] who used it to investigate the climate sensitivity of the CCSM4.

In this study CAM4 and CLM4 are run on the same 2° finite volume grid, while SOM and CICE4 are run on the nominal 1° displaced pole grid. We perform two experiments, each of which is integrated from the same initial condition for 100 years. The control run (cntl) uses the aforementioned default settings and has the annual mean trade winds in the central to eastern tropical Pacific converging to the north of the equator as in observations. The sensitivity run (Qa) is the same as the control run except that a Q_{flux} anomaly is added at

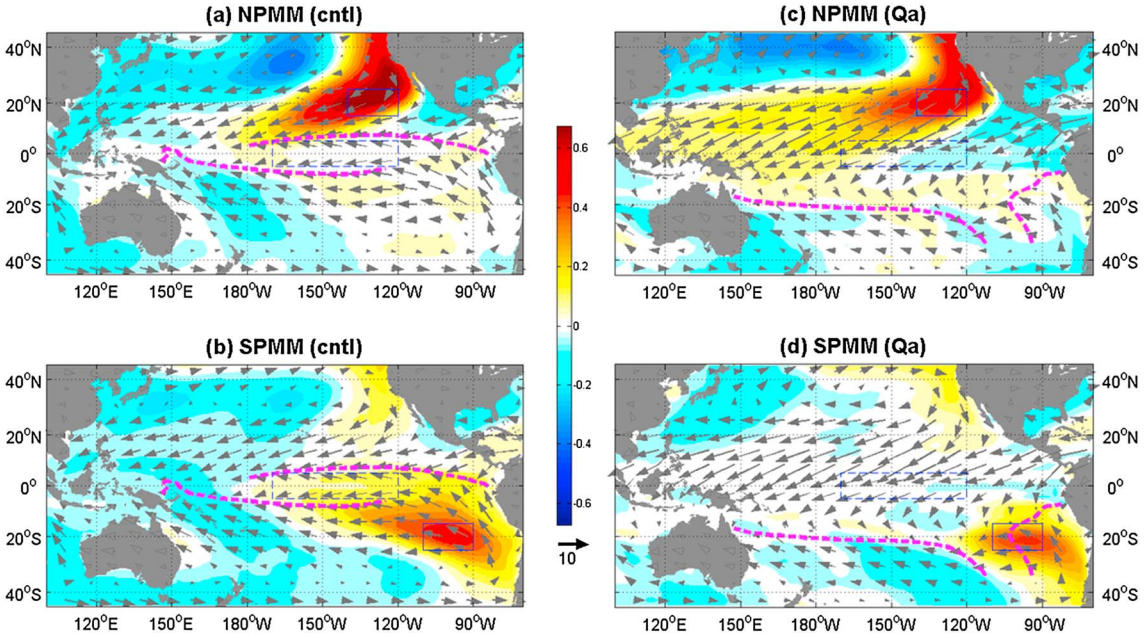

Figure 2. Regression (shading) of SST anomalies onto the anomalous SST time series averaged over the northeast Pacific (15°N–25°N, 140°W–120°W, NEP index indicated by blue boxes) for the NPMM (Figure 2a, cntl; Figure 2c, *Q*a) and over the southeast Pacific (15°S–25°S, 110°W–90°W, SEP index indicated by blue boxes) for the SPMM (Figure 2b, cntl; Figure 2d, *Q*a). Mean surface winds are superimposed as vectors, with the zero contour of mean meridional wind component shown in the dashed magenta curves.

each time step to shift the annual mean ITCZ southward. The imposed Q_{flux} anomaly (Figure 1), which cools the northern ocean and warms the southern ocean, is derived from the Q_{flux} prescribed in the control run in the following manner. We take the zonal mean of the difference between winter (November to January) and summer (May to July) mean Q_{flux} from 40°S to 35°N and multiply it by a factor of 1/3. We find that 1/3 is a reasonable choice that allows the Q_{flux} anomaly to change the mean climate sufficiently while at the same time not to make the solution unstable. A 10° wide blending zone with the Q_{flux} anomaly decreasing poleward sinusoidally to zero is further added to the northern (35°N) and southern (40°S) boundary, respectively. A final adjustment to the Q_{flux} anomaly is applied so that its global mean value is zero (i.e., no net heat is added to the model). In the *Q*a experiment, it takes about 20 years for the mean climate to equilibrate in response to the added Q_{flux} anomaly. In the next section, we will present our results on the basis of the last 80 years of integration from both the cntl and *Q*a experiments.

3. Results

3.1. Climate Model Results

Figure 2 shows the annual mean surface winds in the Pacific for the two experiments. In the cntl experiment, the southeasterly trades cross the equator in the eastern basin and converge with the northeasterly trades at the ITCZ around 7°N (Figures 2a and 2b). In contrast, in the *Q*a experiment, the weakened southeasterly trades are limited to the South Pacific while the strengthened northeasterly trades cross the equator throughout the tropical Pacific, pushing the mean convergence zone to around 20°S (Figures 2c and 2d). This change in the position of the mean convergence zone (and associated precipitation maximum; not shown) affects the structure of the PMMs as discussed next.

One way to visualize the spatial pattern of the PMMs is via linear regression on their subtropical center of action [ZCD13]. Here we illustrate the SPMM and NPMM by regressing monthly SST anomalies (with mean seasonal cycle removed) onto the SST anomaly time series averaged over their subtropical centers of action: the southeast Pacific (SEP: 15°S–25°S, 110°W–90°W) and northeast Pacific (NEP: 15°N–25°N, 140°W–120°W), respectively (Figure 2). The regression is not sensitive to the precise area used for the SST indices. The spatial structure of the PMMs is reproduced by the control CAM4SOM (Figures 2a and 2b), consistent with the multimodel ensemble results in ZCD13 (cf. their Figures 1a and 1b). Both PMMs extend equatorward and westward along the direction of the mean trade winds. In particular, the interhemispheric asymmetry of the

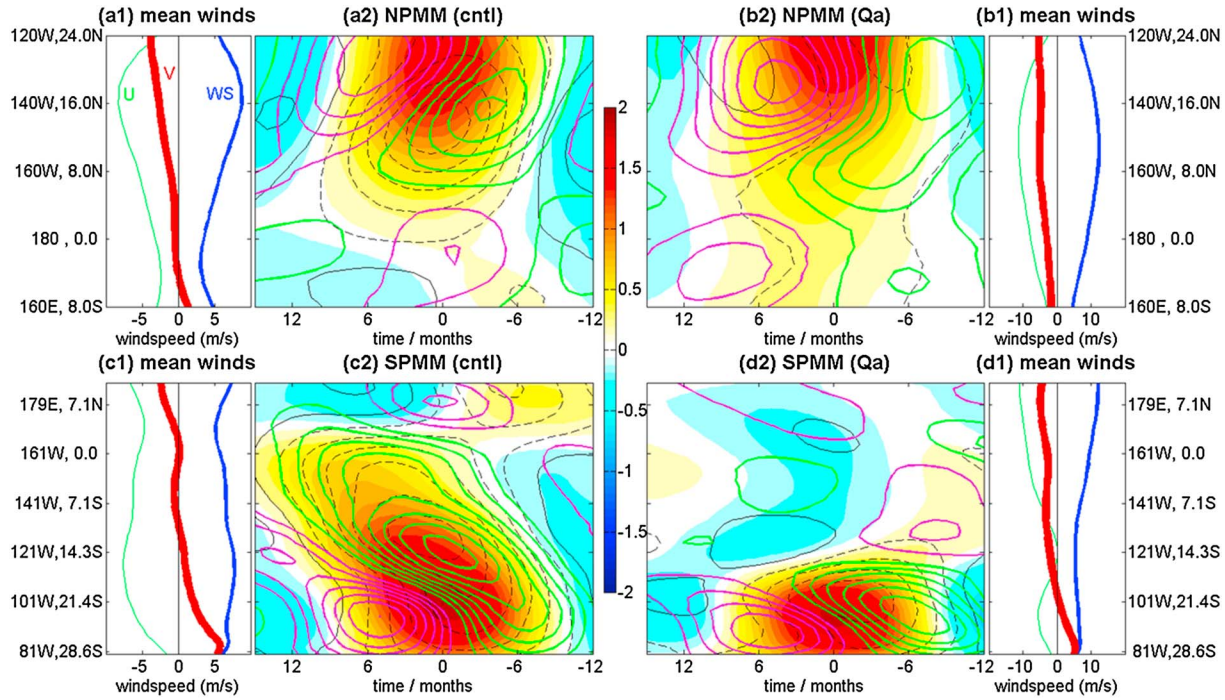

Figure 3. (a1–d1) Mean surface winds and (a2–d2) composite Hovmoller diagrams averaged along the axis of propagation of the NPMM (Figures 3a2 and 3b2) and SPMM (Figures 3c2 and 3d2). The axis of propagation is defined as an 8° wide band with its central axis connecting the endpoints (24°N,120°W) and (8°S, 160°E) for the NPMM and the endpoints (28.6°S, 81°W) and (7.1°N, 179°E) for the SPMM. Results for the cntl and *Qa* experiments are shown in Figures 3a2 and 3c2 and Figures 3b2 and 3d2, respectively. The zonal (green) and meridional (red) components of the mean winds are plotted along with the total wind speed (blue). In the Hovmoller diagrams, thin black contours represent wind speed anomalies (solid for positive, dashed for negative), and thick colored contours represent latent heat flux anomalies (green for downward, magenta for upward). The shading denotes SST anomalies. The composites are based on the NEP index for the NPMM and the SEP index for the SPMM. Note that the time axis goes from right to left.

mean winds appears to be in agreement with the difference between the PMMs: The SPMM has a larger equatorial signature particularly in the eastern-to-central equatorial Pacific where the mean southeasterly trades cross the equator, while the NPMM, with little projection on the equatorial Pacific near dateline, is largely confined to the North Pacific as are the mean northeasterly trades.

In the *Qa* experiment, the spatial pattern of the two PMMs changes dramatically in response to the imposed interhemispheric heating gradient (Figures 2c and 2d). The SST signal associated with the SPMM has a much smaller spatial extent and is completely confined to the southeast subtropical Pacific together with the weakened southeasterly trades (Figure 2d), while that associated with the NPMM has a much larger spatial extent and extends southwestward along the strengthened northeasterly trades with its farthest expansion reaching the western Pacific where the mean northeasterly trades terminate (Figure 2c). Note that the interhemispheric asymmetry between the PMMs in *Qa* is still in agreement with that between the changed mean trade winds, as in the cntl experiment. These consistent changes in the spatial structure of the PMMs and the climatological winds suggest an important role for the mean state in regulating the equatorial linkages of the PMMs.

To show the propagation of the PMMs and their dependence on the mean state, we perform composite analysis for NPMM and SPMM warm events based on the NEP and SEP indices, respectively [ZCD13]. Only included in the composite are the warm events with a peak that is larger than 1 standard deviation of the SST indices. Before conducting the composite, the mean seasonal cycle is removed and a low-pass filter with a cutoff period of 1.5 years is applied to focus on the interannual and decadal time scales (as in ZCD13). Note that the results are not sensitive to the low-pass filter used. Figure 3 shows the composite Hovmoller diagrams plotted along two 8° wide tilted bands selected for the NPMM (Figures 3a2 and 3b2) and the SPMM (Figures 3c2 and 3d2) with their center delineated by the *y* axis. Also plotted in Figure 3 are the mean surface wind speed and its zonal and meridional components along the same bands (Figures 3a1, 3b1, 3c1, and 3d1). In the cntl experiment, the SST signals associated with both the NPMM (Figure 3a2) and SPMM (Figure 3c2) are preceded by weaker wind speeds and positive (downward) latent heat flux anomalies and exhibit clear

Table 1. Parameters Used in the Conceptual Model

Parameter	Definition
f	Coriolis parameter
μ	thermal coupling coefficient
A	atmospheric dissipation coefficient
ρ_o	sea water density
c_p	sea water specific heat
h	slab ocean depth
ρ_a	air density
L_v	latent heat of vaporization
C_E	bulk exchange coefficient

westward-and-equatorward propagation, confirming the WES feedback as the propagating mechanism for the PMMs. For both PMMs, the equatorward propagation is strongly constrained by the mean meridional surface winds: The signals do not propagate beyond the latitude where the mean meridional winds switch direction (Figures 3a1 and 3c1). This is consistent with the asymmetry shown in Figure 2 (left). In the *Q*a case, the propagation associated with the PMMs shows a corresponding change, but the constraint from the mean meridional surface winds still holds. The NPMM propagates to the south of the equator along with the enhanced mean northeasterly trades that continue across the equator (Figures 3b2 and 3b1), while the SPMM exhibits a very weak propagation that stops when the meridional winds switch direction (Figures 3d2 and 3d1). These results from the two experiments suggest that the mean surface winds, particularly their meridional component, exert a dominant constraint on the interhemispheric asymmetry between the NPMM and the SPMM.

3.2. Analytical Model Results

To further explain the constraint from the mean winds, we construct a simple model that couples the Lindzen-Nigam one-layer trade wind boundary layer model used in *Liu and Xie* [1994] with the slab ocean model used in *Wang* [2010]. The governing equations are

$$\begin{cases} -fv = \mu T_x - Au \\ fu = \mu T_y - Av \\ T_t = -Q_{\mathrm{LH}}/\rho_o h c_p \end{cases} \tag{1}$$

where state variables u, v, and T are the zonal, meridional surface winds, and SST, respectively. Other parameters are listed in Table 1. As in *Wang* [2010], we only consider the latent heat flux (positive upward): $Q_{\mathrm{LH}} = \rho_a L_v C_E U(q_s - q)$, where U is the wind speed ($\sqrt{u^2+v^2}$) and $q_{(s)}$ is the (saturated) specific humidity at reference height. Separating the variables into mean and perturbation parts ($X = \overline{X} + X'$) and linearizing equations (1) around the mean, one obtains the equations for perturbation (primes dropped)

$$\begin{cases} -fv = \mu T_x - Au \\ fu = \mu T_y - Av \\ T_t = -a(\overline{u}u + \overline{v}v)/\overline{U} - bT \end{cases} \tag{2}$$

where $a = \frac{\rho_a L_v C_E}{\rho_o h c_p}(\overline{q}_s - \overline{q})$, $b = a\frac{L_v \overline{U}}{R_v \overline{T}^2}$ and note $a \geq 0, b \geq 0$. Combing these three equations by eliminating u and v, one obtains a single SST equation for the coupled system

$$T_t + C_x T_x + C_y T_y = -bT \tag{3}$$

where

$$\begin{aligned} C_x &= \frac{a\mu}{\overline{U}(f^2 + A^2)}(A\overline{u} - f\overline{v}) \\ C_y &= \frac{a\mu}{\overline{U}(f^2 + A^2)}(f\overline{u} + A\overline{v}) \end{aligned} \tag{4}$$

Equation (3) is a first-order partial differential equation, with its left-hand side representing nondispersive two-dimensional waves propagating at the total wave speed (C_x, C_y) along the characteristic delineated by

$$\begin{aligned} \frac{dt}{ds} &= 1 \\ \frac{dx}{ds} &= C_x \\ \frac{dy}{ds} &= C_y \end{aligned}$$

The SST anomaly evolves along this characteristic following $\frac{dT}{ds} = -bT$. This propagation is fundamentally due to the WES feedback. As can be seen from expression (4), the meridional wave speed C_y depends on both

components of the mean winds. In the tropics where easterlies prevail ($\overline{u} < 0$), the meridional propagation related with $\overline{u}$ is equatorward and switches direction at the equator ($C_y(\overline{u}) = \frac{a\mu}{\overline{U}\left(f^2+A^2\right)} f\overline{u} \sim -f$, note $\frac{a\mu}{\overline{U}\left(f^2+A^2\right)} \geq 0$). In contrast, the meridional propagation related with $\overline{v}$ follows the mean meridional winds ($C_y(\overline{v}) = \frac{a\mu}{\overline{U}\left(f^2+A^2\right)} A\overline{v} \sim \overline{v}$), so that cross-equatorial mean meridional winds will lead to cross-equatorial propagation of the SST anomalies [see *Liu and Xie*, 1994, Figure 3]. Therefore, it is the mean meridional winds that are responsible for the interhemispheric asymmetry between the PMMs by influencing the WES feedback.

4. Summary and Discussion

ZCD13 have recently shown that the South Pacific has a stronger coupling to the equatorial Pacific via the SPMM than the North Pacific via the equivalent NPMM and hypothesized that this difference is due to the asymmetric distribution of mean trade winds in the tropical Pacific. In this study we test this hypothesis by first modifying the mean surface wind distribution in CAM4SOM and then examining the consequent changes in the PMMs.

Specifically, we shift the ITCZ to the south of the equator by cooling the Northern Hemisphere and warming the Southern Hemisphere. With this new climate state, the spatial pattern of the SPMM is completely confined to the South Pacific while that of the NPMM expands to the central-western equatorial Pacific. These spatial changes in the PMMs are in agreement with those in the mean surface winds. Further analysis demonstrates that the propagation of the PMMs changes correspondingly, with a strong constraint from the mean surface winds. The equatorward propagation of both PMMs cannot go beyond the location of the mean convergence zone where the mean meridional winds change direction. These results suggest that the changes in the PMMs are attributable to the changes in the mean trade winds. The strengthened northeasterly trades which extend across the equator provide the necessary condition for the NPMM to propagate into the Southern Hemisphere, while the suppressed mean southeasterly trades remove the same necessary condition for the SPMM to reach the equator. In both cases, the fundamental reason is the dependence of the WES feedback on the background surface winds. We demonstrate this dependence with a conceptual model constructed by coupling a Lindzen-Nigam type atmosphere model to a slab ocean model, similar to the study of *Liu and Xie* [1994]. Therefore, we conclude that the mean surface winds in the tropical Pacific, particularly their meridional component, impose a dominant constraint on the equatorial influence of the PMMs, and their asymmetric distribution largely accounts for the interhemispheric asymmetry between PMMs.

However, there are some changes of the PMMs between the cntl and *Q*a experiments that cannot be explained by the mean wind constraint. For instance, in the eastern equatorial Pacific, the NPMM in the *Q*a experiment does not show any response to the changes in the northeasterly trades (Figure 2a versus 2c). This may be related to the orientation of the coastline which keeps the North Pacific Oscillation (the extratropical driver of the NPMM) from extending southeastward toward the eastern equatorial Pacific. In the western Pacific, the two PMMs in the cntl experiment do not extend as far west as the mean surface winds (Figures 2a and 2b). This is likely attributable to the damping from high-level clouds [ZCD13].

This study employs a slab ocean model configuration that excludes active ocean dynamics and ocean-atmosphere dynamical feedback. Nonetheless, ZCD13 have shown that the interhemispheric asymmetry between the PMMs is a robust feature not only in AGCM-slab models but also in fully coupled climate models (and observations). Although not required by the physics of the PMMs, ocean dynamics and associated feedback may contribute to the interhemispheric asymmetry between the PMMs either directly via meridional ocean advection [*Liu and Xie*, 1994] or indirectly by influencing the climatological surface winds. The role of ocean dynamics is left to future work.

This study has implications for understanding the role of mean climate in regulating internal climate variability. For example, our results suggest that the connections from the extratropics to the tropics may vary over glacial and interglacial periods when the interhemispheric contrast and cross-equatorial winds were significantly different from modern climate [*Timmermann et al*., 2007; *DiNezio et al*., 2011]. From the modeling development perspective, our work suggests that resolving issues in the simulation of the mean state, such as the "cold tongue" and "double-ITCZ" biases, in the current generation of climate models (including the one used here) may influence, and potentially improve, the simulation of climate variability associated with the PMMs.

Acknowledgments

We would like to acknowledge the high-performance computing support from Yellowstone (ark:/85065/d7wd3xhc) provided by NCAR's *Computational and Information Systems Laboratory* [2013], sponsored by the National Science Foundation. We would also like to thank the Advanced Study Program at NCAR for the financial support for H.Z.'s visit at NCAR during which this work has been conducted. Comments from two anonymous reviewers help to improve the manuscript. NCAR is supported by the National Science Foundation. H.Z. and A.C.C. were supported by grants from the NSF Climate and Large-scale Dynamics program, the NOAA Climate Program Office, and the DOE Biological and Environmental Research Program.

The Editor thanks two anonymous reviewers for assistance in evaluating this paper.

References

Bitz, C. M., K. M. Shell, P. R. Gent, D. A. Bailey, G. Danabasoglu, K. C. Armour, M. M. Holland, and J. T. Kiehl (2012), Climate sensitivity of the Community Climate System Model, Version 4, *J. Clim.*, *25*(9), 3053–3070.

Chang, P., L. Ji, and H. Li (1997), A decadal climate variation in the tropical Atlantic Ocean from thermodynamic air–sea interactions, *Nature*, *385*, 516–518.

Chang, P., L. Zhang, R. Saravanan, D. J. Vimont, J. C. H. Chiang, L. Ji, H. Seidel, and M. K. Tippett (2007), Pacific meridional mode and El Nino–Southern Oscillation, *Geophys. Res. Lett.*, *34*, L16608, doi:10.1029/2007GL030302.

Chiang, J. C. H., and D. J. Vimont (2004), Analogous Pacific and Atlantic meridional modes of tropical atmosphere–ocean variability, *J. Clim.*, *17*, 4143–4158.

Clement, A. C., P. DiNezio, and C. Deser (2011), Rethinking the ocean's role in the Southern Oscillation, *J. Clim.*, *24*, 4056–4072.

Computational and Information Systems Laboratory (2013), Yellowstone: IBM iDataPlex System (NCAR Community Computing), http://n2t.net/ark:/85065/d7wd3xhc, Natl. Cent. Atmos. Res., Boulder, Colo.

DiNezio, P. N., A. Clement, G. A. Vecchi, B. Soden, A. J. Broccoli, B. L. Otto-Bliesner, and P. Braconnot (2011), The response of the Walker circulation to Last Glacial Maximum forcing: Implications for detection in proxies, *Paleoceanography*, *26*, PA3217, doi:10.1029/2010PA002083.

Gent, P., et al. (2011), The Community Climate System Model, version 4, *J. Clim.*, *24*, 4973–4991.

Kossin, J. P., and D. J. Vimont (2007), A more general framework for understanding Atlantic hurricane variability and trends, *Bull. Am. Meteorol. Soc.*, *88*, 1767–1781.

Liu, Z., and S.-P. Xie (1994), Equatorward propagation of coupled air–sea disturbances with application to the annual cycle of the eastern tropical Pacific, *J. Atmos. Sci.*, *51*, 3807–3822.

Matei, D., N. Keenlyside, M. Latif, and J. Jungclaus (2008), Subtropical forcing of tropical Pacific climate and decadal ENSO modulation, *J. Clim.*, *21*, 4691–4709.

Nobre, P., and J. Shukla (1996), Variations of sea surface temperature, wind stress, and rainfall over the tropical Atlantic and South America, *J. Clim.*, *9*, 2464–2479.

Okumura, Y. M. (2013), Origins of tropical Pacific decadal variability: Role of stochastic atmospheric forcing from the South Pacific, *J. Climate*, *26*, 9791–9796, doi:10.1175/JCLI-D-13-00448.1.

Timmermann, A., et al. (2007), The influence of a weakening of the Atlantic meridional overturning circulation on ENSO, *J. Clim.*, *20*, 4899–4919, doi:10.1175/JCLI4283.1.

Wang, F. (2010), Thermodynamical coupled modes in the tropical atmosphere-ocean: An analytical solution, *J. Atmos. Sci.*, *67*, 1667–1677.

Xie, S.-P., and S. G. H. Philander (1994), A coupled ocean-atmosphere model of relevance to the ITCZ in the eastern Pacific, *Tellus*, *46A*, 340–350.

Xie, S.-P., and Y. Tanimoto (1998), A pan-Atlantic decadal climate oscillation, *Geophys. Res. Lett.*, *25*, 2185–2188.

Zhang, H., A. Clement, and P. DiNezio (2014), The South Pacific meridional mode: A mechanism for ENSO-like variability, *J. Clim.*, *27*, 769–783, doi:10.1175/JCLI-D-13-00082.1.